Acrylamide-Based Magnetic Nanosponges: A New Smart Nanocomposite Material

ARTICLE *in* LANGMUIR · NOVEMBER 2008

Impact Factor: 4.46 · DOI: 10.1021/la802425k · Source: PubMed

8 AUTHORS, INCLUDING:

Massimo Bonini
University of Florence
60 PUBLICATIONS **1,547** CITATIONS
SEE PROFILE

Francesca Ridi
University of Florence
40 PUBLICATIONS **510** CITATIONS
SEE PROFILE

Emiliano Carretti
University of Florence
59 PUBLICATIONS **793** CITATIONS
SEE PROFILE

Piero Baglioni
University of Florence
448 PUBLICATIONS **8,083** CITATIONS
SEE PROFILE

Langmuir

Article

Acrylamide-Based Magnetic Nanosponges: A New Smart Nanocomposite Material

Massimo Bonini, Sebastian Lenz, Ester Falletta, Francesca Ridi, Emiliano Carretti, Emiliano Fratini, Albrecht Wiedenmann, and Piero Baglioni

Langmuir, **2008**, 24 (21), 12644-12650 • DOI: 10.1021/la802425k • Publication Date (Web): 10 October 2008

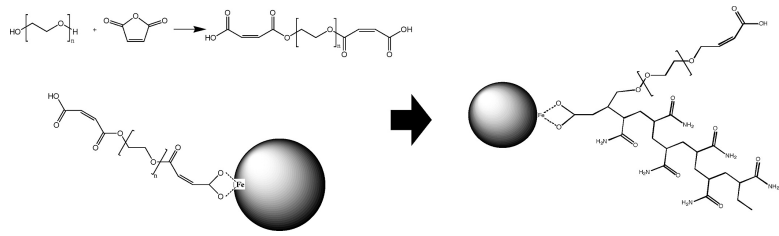

More About This Article

Additional resources and features associated with this article are available within the HTML version:

- Supporting Information
- Access to high resolution figures
- Links to articles and content related to this article
- Copyright permission to reproduce figures and/or text from this article

View the Full Text HTML

Acrylamide-Based Magnetic Nanosponges: A New Smart Nanocomposite Material

Massimo Bonini,[†,#] Sebastian Lenz,[†,§] Ester Falletta,[†] Francesca Ridi,[†] Emiliano Carretti,[†] Emiliano Fratini,[†] Albrecht Wiedenmann,[‡] and Piero Baglioni*[,†]

Department of Chemistry and CSGI, University of Florence, via della Lastruccia 3 - 50019 Sesto Fiorentino, Florence, Italy, and Hahn-Meitner-Institut, Glienicker Strasse 100, D-14109 Berlin, Germany

Received July 28, 2008

Nanocomposite materials consisting of $CoFe_2O_4$ magnetic nanoparticles and a polyethylene glycol−acrylamide gel matrix have been synthesized. The structure of such materials was studied by means of small-angle scattering of X-rays and polarized neutrons, showing that the $CoFe_2O_4$ nanoparticles were successfully and homogeneously embedded in the gel structure. Magnetic, viscoelastic, and water retention properties of the nanocomposite gel confirm that the properties of both nanoparticles and gel are combined in the resulting nanomagnetic gel. Scanning electron microscopy highlights the nanocomposite nature of the material, showing the presence of a gel structure with different pore size distributions (pores with micron and nano-size distributions) that can be used as active sponge-like nanomagnetic container for water-based formulations as oil-in-water microemulsions.

Introduction

Nanocomposite materials have recently been shown to represent a powerful approach in the preparation of functional materials.[1,2] In particular, polymeric nanocomposites where a polymer matrix is combined with inorganic nanoparticles have gathered much attention during the past years.[1,3−5] The size and properties of polymers make them a convenient scaffold to disperse and arrange other nanoscaled objects to produce nanocomposites with enhanced properties. In particular, nanocomposites consisting of a polymeric network that embeds magnetic nanoparticles (MagNPs) represent a feasible approach in the preparation of magnetic gels.[6−9] In this context, the research of materials able to combine the peculiar properties of both permanent hydrogels and MagNPs is an important step in the formulation of smart functional materials.

In this contribution we report in detail the synthesis and the characterization of a gel that is able to load a large amount of water-based formulations, with a structure that can be modified and adapted to specific functions. In view of synthesizing a permanent hydrogel, where MagNPs are chemically connected to the network structure, basic requirements should be addressed. First, the gel structure should be capable to load as much water as possible. Therefore we choose an acrylamide-based gel formulation, as the water-loading properties of acrylamide are known to be very good. Second, in order to connect the acrylamide network to the MagNPs, we used a strategy similar to that previously reported by Gupta and Wells.[10] To this purpose, a polymerizable polyethylene glycol (PEG)-derivative was prepared by esterification of PEG with maleic anhydride (MA). The PEG backbone was chosen because of its hydrophylicity. The complete esterification with MA leads to the formation of a linear polymer where two carboxylic moieties are introduced at both endings of the chain, together with two double bonds that represent the polymerizable groups (see the Experimental Section for further details). The carboxylic groups are then used to link the MagNPs to the PEG-derivative: in fact, the binding reaction between MagNPs and carboxylic acids is well-known to take to a complete coupling of the carboxylic headgroup onto the surface of the particles.[11] On the other hand, the double bonds were used to incorporate the MagNP−PEG adducts into the polyacrylamide gel network, which was obtained by polymerizing acrylamide and *N*,*N*′-methylene bisacrylamide.

Following this approach, we successfully prepared nanocomposite materials that combine the properties of permanent hydrogels to those of magnetic responsive nanoparticles, called hereinafter nanomagnetic sponges. The structure was studied by using small-angle X-ray scattering (SAXS) and small-angle neutron scattering of polarized neutrons (SANSPOL). Furthermore, we showed by scanning electron microscopy (SEM) that these nanomagnetic sponges can be used as active containers for water-based formulations. To this purpose we uploaded an oil-in-water microemulsion (μE) into the porous structure of the magnetic hydrogel and we showed that the μE can also be released in the presence of an external magnetic stimulus. An example of the potentialities of these new materials has been recently reported in the context of the Conservation of Cultural Heritage.[8]

Experimental Section

Nanomagnetic Gel Synthesis. As outlined in the Introduction, a PEG-derivative was properly synthesized to embed the MagNPs into the acrylamide gel structure. Chloroform (200 mL, HPLC grade,

* Corresponding author. Phone: +39 055 457-3033. Fax: +39 055 457-3032. E-mail: baglioni@csgi.unifi.it. URL: www.csgi.unifi.it.
† University of Florence.
‡ Hahn-Meitner-Institut.
# Present address: BASF SE, 67056 Ludwigshafen, Germany.
§ Present address: Max Planck Institute for Polymer Research, Ackermannweg 10, D-55128 Mainz, Germany.

(1) Mark, J. E. *Acc. Chem. Res.* **2006**, *39*, 881–888.
(2) Hussain, F.; Hojjati, M.; Okamoto, M.; Gorga, R. E. *J. Compos. Mater.* **2006**, *40*, 1511–1575.
(3) Bourgeat-Lami, E. *J. Nanosci. Nanotechnol.* **2002**, *2*, 1–24.
(4) Shenhar, R.; Rotello, V. M. *Acc. Chem. Res.* **2003**, *36*, 549–561.
(5) Pomogailo, A. D.; Kestelman, V. N. *Metallopolymer Nanocomposites*; Springer Verlag: Berlin, 2005.
(6) Francois, N. J.; Silvia, S. A.; Jacobo, E.; Daraio, M. E. *J. Appl. Polym. Sci.* **2007**, *105*, 647–655.
(7) Millan, A.; Palacio, F.; Snoeck, E.; Serin, V.; Lecante, P. In *Polymer Nanocomposites*; Mai, Y.-W., Yu, Z.-Z., Eds.; Woodhead Publishing Limited: Cambridge, U.K., 2006.
(8) Bonini, M.; Lenz, S.; Giorgi, R.; Baglioni, P. *Langmuir* **2007**, *23*, 8681–8685.
(9) Hernández, R.; López, G.; Lópeza, D. *J. Mater. Res.* **2007**, 22.
(10) Gupta, A. K.; Wells, S. *IEEE Trans. Nanobiosci.* **2004**, *3*, 66–73.
(11) Sartoratto, P. P. C.; Neto, A. V. S.; Lima, E. C. D.; Rodrigues de Sá, A. L. C.; Morais, P. C. *J. Appl. Phys.* **2005**, *97*, 10Q917.

10.1021/la802425k CCC: $40.75
Published on Web 10/10/2008

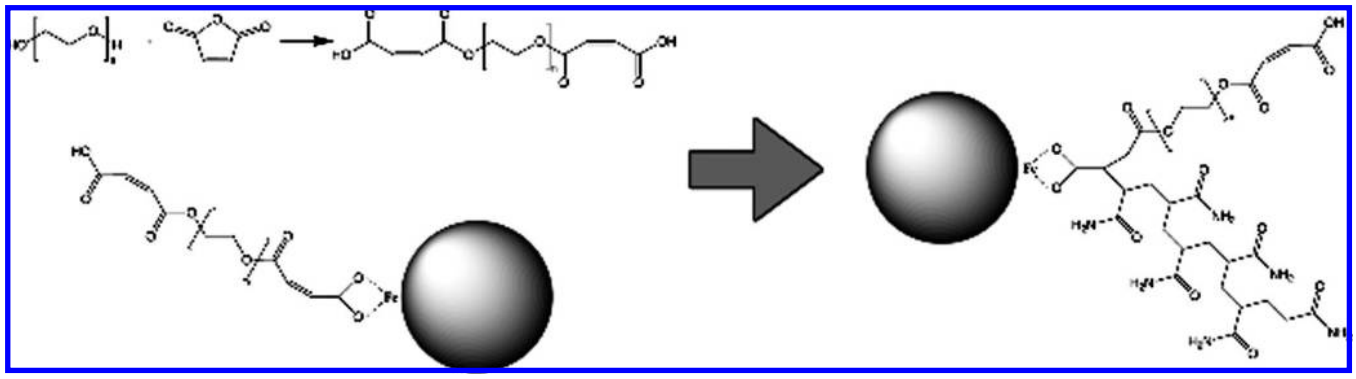

Figure 1. Scheme of the reaction between ethylene glycol and MA (top-left) and sketch of coupling between the surface of MagNP and the ethylene glycol dicarboxyl derivative (bottom-left). The right panel shows the magnetic particle cross-linked to the acrylamide gel chains.

99.9% purity, obtained from Aldrich, Milan) was deoxygenated through Argon purging for 15 min. Twenty grams of Polyethylene glycol (0.1 mol, $M_w \approx 200$ g/mol, Sigma, Milan) was added together with 19.6 g of MA (Sigma, Milan) still under Argon purging. The reaction was then carried out in the dark for 24 h at 37 °C. During the reaction, two ester bonds are formed as a result of the chemical reaction between the MA anhydride group and the hydroxyl groups of PEG (see Figure 1). Thereinafter, we will refer to the obtained product as MA−PEG−MA.

MagNPs were synthesized as already reported in detail elsewhere.[12−16] A stable ferrofluid consisting of positively charged $CoFe_2O_4$ nanoparticles dispersed in water was obtained. The concentration of nanoparticles was adjusted to 1% w/w to obtain the ferrofluid used throughout the rest of the synthesis (referred to as FF). The size and polydispersity of the nanoparticles agreed with a previous nanoparticle batch that was previously investigated,[14] showing a mean diameter of about 8 nm and a polydispersity of about 0.4.

A solution of MA−PEG−MA was prepared by dissolving 0.5 g in 10 mL of water. This solution was then added to the FF (5 mL, 0.5 g of MagNP), and the mixture was sonicated for 15 min (Eurosonic 22). In this step, as outlined in the Introduction, the carboxylic groups react with the surface of the nanoparticles to form a slightly viscous magnetic fluid (see Figure 1).[11]

Separately, a clear solution containing 0.75 g of acrylamide (Fluka, Milan, purity ≥99%) and 60 mg of *N*,*N*′-methylene bisacrylamide (Fluka, Milan, purity ≥98%) in 10 mL of water was prepared.

The acrylamide solution and magnetic fluid were then purged with N_2 and mixed together. Ammonium persulfate (Aldrich, Milan, purity >98%) was then added as a radical initiator, and the reaction was carried out at 42 °C for 4 h. Throughout the rest of the paper we will refer to the sample prepared by means of such procedure as MagGel. In order to check the effect of the stirring over the obtained gel structure, one sample was polymerized without any mixing (hereinafter referred to as NS-MagGel). A reference gel (RefGel) containing no MagNPs was prepared as well.

At the end of the polymerization, a magnetic black gel is obtained in the cases of the samples containing MagNPs, while the reference gel is slightly opalescent. Only in the case of gel prepared without stirring, phase separation was observed, with one fluid phase on top containing nonmagnetic particles and a gel-phase on the bottom containing almost the totality of magnetic particles. Pristine gels showed a pH of ∼1. In order to increase the pH, each gel was washed, at least 10 times, with a large excess of water (purified by a Millipore Organex system; $R \geq 18$ MΩ cm) until a pH of 4 was reached.

The stability of the hydrogels was checked by freeze-drying the hydrogels to xerogels and rehydrating them in an excess of water. Lyophilized gels return to the completely swollen state in a few minutes. As usual for permanent gels, this process can be repeated several times without any detectable change in the structure.

Similarly to a xerogel, the reference gel is a porous white powder, while gels containing cobaltferrite nanoparticles appear homogeneously black.

Dehydration Tests. In order to evaluate hydrophilic properties of the gels, a known amount of the freeze-dried xerogel was fully hydrated by dipping it in water for a few minutes. We found that, in both the reference and the magnetic gels, the maximum amount of loaded water was slightly higher than 90% by weight of the final hydrated sample. In order to investigate the differences between the gels' behavior, xerogels were first hydrated with a known amount of water (90 wt % of water, 10 wt % of freeze-dried powder). Then they were stored in a controlled humidity chamber (50% relative humidity), and their weight was checked during the following 30 days.

Rheology. Oscillatory shear measurements were conducted on a Paar Physica UDS 200 rheometer working in controlled shear stress equipped with a 1° cone and plate geometry of 25 mm diameter. The dependence of the rheological parameters G', G'', and η^* from the oscillation frequency (ϖ) was obtained from the phase lag between the applied shear stress and the related flow and from the ratio between the amplitudes of the imposed oscillation and the response of the gel. The complex viscosity is given by

$$|\eta^*(\varpi)| = \sqrt{\frac{G'^2(\varpi) + G''^2(\varpi)}{\varpi^2}} \qquad (1)$$

The storage modulus (G') and the loss modulus (G'') were measured over the frequency range 0.001−50 s^{-1}. The values of the stress amplitude were checked by means of an amplitude sweep test in order to ensure that all measurements were performed within the linear viscoelastic region.

All the samples were equilibrated for 1 h at 20 °C before the experiments. All the measurements were performed at a temperature of 20.00 ± 0.01 °C (Peltier temperature control system).

With regards to the gel preparation, it is important to state that is impossible to finely tune the water content in the investigated samples: in fact, when the conically shaped measurement head approaches the gel deposited onto the plate, the material is partially squeezed out from the head−plate gap and, at the same time, a minimum amount of water is released from the gel network. This makes it impossible to exactly know the real water content. Nevertheless, in order to make the measurements reliable, we always used the same amount of fully hydrated sample on the plate, and we always maintained the same measurement conditions. All measurements were repeated at least five times in order to obtain a good reproducibility.

(12) Massart, R. *C. R. Hebd. Seances Acad. Sci., Ser. C* **1980**, *291*, 1–3.
(13) Massart, R. *IEEE Trans. Magn.* **1981**, *17*, 1247–1248.
(14) Bonini, M.; Wiedenmann, A.; Baglioni, P. *J. Phys. Chem. B* **2004**, *108*, 14901–14906.
(15) Bonini, M.; Wiedenmann, A.; Baglioni, P. *Physica A* **2004**, *339*, 86–91.
(16) Bonini, M.; Wiedemann, A.; Baglioni, P. *Mater. Sci. Eng. C: Biomimetic Supramol. Syst.* **2006**, *26*, 745–750.

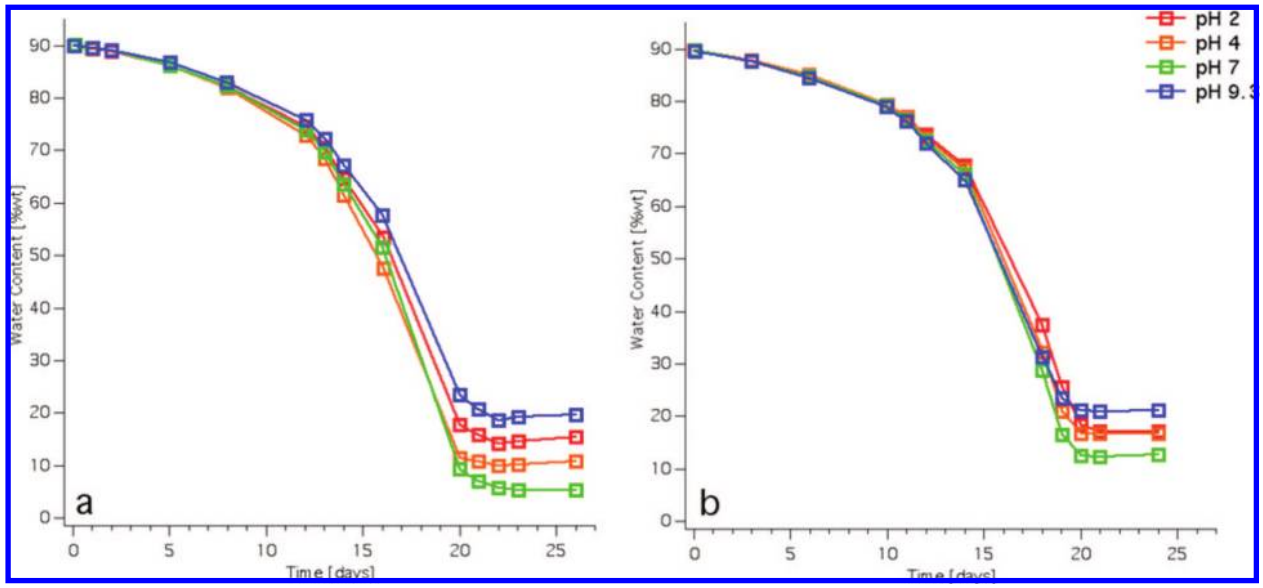

Figure 2. Dehydration curves of samples RefGel (a) and MagGel (b) at different pH values.

SANSPOL. SANSPOL measurements were carried out to investigate the nanostructure of the magnetic gel. In this particular case, the xerogel sample was rehydrated with D_2O (Eurisotop, Saclay, France) in order to maximize the contrast between the "solvent" and the gel network and to minimize the incoherent background contribution. SANSPOL experiments were performed at the V4 instrument at the BERII reactor of the Hahn-Meitner Institute, Berlin. A horizontal magnetic field (about 1 T) was applied at the sample position, oriented perpendicularly to the incoming neutrons. Polarized neutrons are provided by a transmission polarizing supermirror cavity. The polarization direction is reversed using a spin flipper in front of the sample. Data were reduced to absolute intensities according to the conventional method used at HMI by using the BerSANS-PC software package.[17]

SAXS. The measurements were carried out with a Nanoviewer (Rigaku), equipped with a Mercury70 Charge Coupled Device detector (1024 × 1024 pixels, pixel dimension: 68 μm). Cu Kα radiation (λ = 1.5418 Å) was provided by a Micromax007 X-ray rotating anode (Rigaku), operating at a maximum power of 0.8 kW with a focal spot diameter of 70 μm. X-rays were conditioned using a Confocal Max-Flux Mirror (Rigaku/Osmic) in order to totally remove the Cu K_β maintaining the high flux and symmetry of the rotating anode source. X-ray collimation was performed through a three-point collimation system. The sample-to-detector distance was about 605 mm. The volume between the sample and the detector was kept under vacuum during the measurements to minimize scattering from the air. The Q-range was calibrated using silver behenate, which is known to have a well-defined lamellar structure (d = 58.48 Å)[18] where the scattering vector Q is defined as $Q = 4\pi/\lambda \sin(\theta/2)$, with θ being the scattering angle. Scattering curves were monitored in a Q-range from 0.01 to 0.3 $Å^{-1}$. The gel samples were filled into a demountable solid samples holder consisting of two thin Kapton windows and a 1 mm stainless steel spacer. The experimental temperature (25 °C) was controlled by a Peltier element, with an accuracy of ± 0.1 °C. All two-dimensional (2D) spectra were corrected for the dark current, and a dezingering procedure was applied to all images in order to remove spurious signals. The empty cell contribution (Kapton windows) was subtracted using the empty cell/sample transmission ratios. Finally, 2D spectra were azimuthally averaged in order to obtain the correspondent one-dimensional (1D) scattering intensity distribution.

SEM. SEM observations were carried out by means of a Cambridge Stereoscan 360S, working at 25 kV of acceleration potential, with a working distance of 25 mm. Few milligrams of the xerogel were deposited onto the stub and coated with a gold film (Agar automatic sputter coater) in order to make the sample conductive.

Table 1. Final Water Content Values for the Gel at Three Different pH Values

	water [%wt]			
sample	pH 2	pH 4	pH 7	pH 9.3
RefGel	15.6	11.1	5.6	20.0
MagGel	17.0	16.6	12.6	20.9

Results and Discussion

Dehydration Behavior. Dehydration curves are shown in Figure 2 for RefGel (a) and MagGel (b). As the gels have a polyelectrolyte nature (amidic and carboxylic groups are present in large amount), the dependency of the dehydration behavior against the pH was considered. Four different pH values were investigated: 2, 4, 7, and 9.3 (pH was adjusted by washing the gel in NaOH water solution). We note that all the dehydration curves show a similar behavior, with a nearly linear water loss during the first 10 days, followed by a faster decrease during the next week, ending in a plateau after about 20 days. The presence of MagNPs only slightly changes the water retention properties of the gel structure that can be evidenced in the final part of the curves (see Table 1).

Let us first discuss the behavior of the sample RefGel. It is well-known that the swelling properties of polyacrylamide-based gel[19] dramatically depend on the pH: in particular, the gel structure at neutral pH is largely more swollen than at acid or alkaline pH. On the other hand, the water still bound to the gel network after about 1 month consists of molecules trapped in smaller pores, since most of the water has been already released from the large pores. One should expect that pores size is strictly related to the swollen degree of the gel (that, in the present case, depends on the pH) and, consequently, the lower amount in the final water content fairly explains the results found at pH 7, that is, the pH where the gel is more swollen.

MagNPs introduced in the gel structure influence the water retention properties depending on the pH. At pH 2 and 9.3, the

(17) Keiderling, U. *Appl. Phys. A: Mater. Sci. Process.* **2002**, *74*, s1455−s1457.
(18) Blanton, T.; Huang, T. C.; Toraya, H.; Hubbard, C. R.; Robie, S. B.; Louer, D.; Gobel, H. E.; Will, G.; Gilles, R.; Raftery, T. *Powder Diffr.* **1995**, *10*, 91–95.
(19) Gemeinhart, R. A.; Guo, C. In *Reflexive Polymers and Hydrogels*; CRC Press, LLC: Boca Raton, FL, 2004, pp 245−257.

samples show quite similar values, while at pH 4 and, in particular, at pH 7, a clear dependency on the MagNP content is present. This is due to the "structuring effect" of the nanoparticles over the gel structure: i.e., each nanoparticle acts as an anchoring point for the PAAm/PEO. The part of the gel located in the proximity of the particles cannot be swollen as in the reference gel. As a consequence, the size of the pores situated in these regions is not really affected by the pH, since their local structure is dictated by steric constrictions. It is important to stress that this effect can not be ascribed to a charge effect of the nanoparticles: in fact, the point of zero charge (PZC) of the MagNP surface is around pH 7.[20] Moreover, the MagNP surface is coated with the carboxylic acid moieties during the condensation reaction.

SANSPOL. More insight into the nanocomposite gel structure was obtained through SANSPOL experiments. This technique has already been proven very useful to explore MagNPs.[14,15,21−24] The sample investigated by SANSPOL was prepared as described for sample MagGel in the Experimental Section, freeze-dried, and then the xerogel was rehydrated with fully deuterated water (80% by weight of D_2O, 20 wt % of gel powder).

In Figure 3 (top) the results for the nonpolarized intensity are shown, while, in the bottom, the SANSPOL intensities are shown together with the fitting results. The scattering behavior of gels formed from gelatin has been deeply investigated in the past.[25−28] It has been shown that the total intensity arising from a gelatin can be considered as the sum of two contributions (see below). In our case, because of the presence of MagNPs, a third component should be considered:

$$I(Q) = I_{\text{Lorentz}}(Q) + I_{\text{excess}}(Q) + I_{\text{MagNP}}(Q) + \text{bkg} \qquad (2)$$

where bkg is the incoherent background.

The scattering intensity due to the MagNPs (I_{MagNP} (Q)) was modeled according to the formalism introduced by Bartlett and Ottewill for polydisperse spherical particles.[29] In this approach, the particles are described as spherical objects with a Schulz distribution of radii.[30,31] More details about the fitting procedure are available in the Supporting Information. Here it is important to stress that the parameters obtained from the fitting are the volume fraction of the MagNPs, their average radius and polydispersity, and both particles' nuclear and magnetic scattering length densities (SLDs).

The Lorentzian component can be described as

$$I_{\text{Lorentz}}(Q) = \frac{I_{\text{Lorentz}}(0)}{1 + Q^2\xi^2} \qquad (3)$$

where $I_{\text{Lorentz}}(0)$ is the Lorentzian intensity at $Q = 0$, Q is the scattering vector, and ξ is the mesh size of the gel network.

According to the Debye−Bueche theory,[26] an excess scattering term has to be introduced to account for the inhomogeneities:[28]

$$I_{\text{excess}}(Q) = \frac{I_{\text{excess}}(0)}{(1 + Q^2a^2)^2} \qquad (4)$$

where $I_{\text{excess}}(0)$ is the Debye−Bueche intensity at $Q = 0$, and a is the inhomogeneity domains' size.

As mentioned in the Experimental Section, the SANSPOL technique allows the separation of the nuclear and magnetic contributions to the scattering intensity. In the case of our gel, the magnetic content is quite low, as only 20 wt % consists of polymer and magnetic particles. This is consistent with the small variations between the nonpolarized and the flipper ON and OFF polarized intensities (see Figure 3). Nevertheless, this small variation allows for the simultaneous fitting of the structural parameters of both the MagNPs and the gel network.

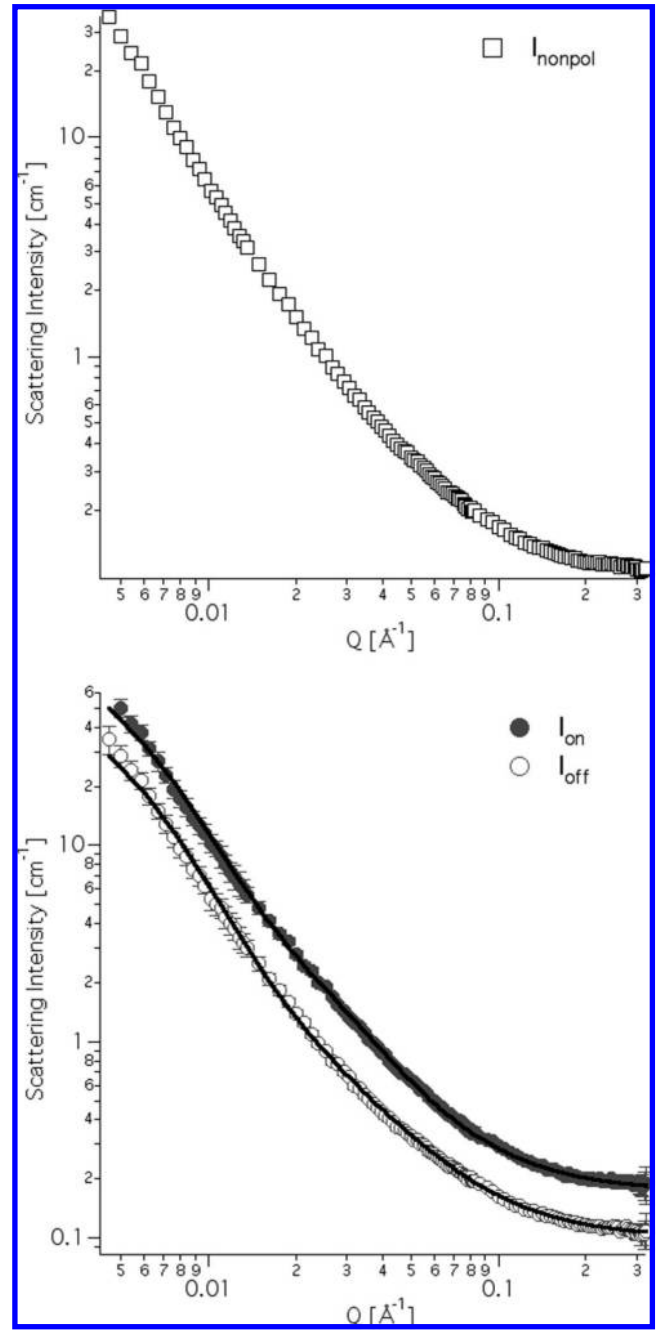

Figure 3. SANS (top) and SANSPOL (bottom) intensities of the MagGel sample together with the fit results (black solid lines). For the sake of clarity, in the bottom panel, I_{on} and the relative fit were offset by 5 cm^{-1}.

(20) Tourinho, F. A.; Campos, A. F. C.; Aquino, R.; Lara, M. C. F. L.; da Silva, G. J.; Depeyrot, J. *Braz. J. Phys.* **2002**, 32.
(21) Wiedenmann, A. *J. Appl. Crystallogr.* **2000**, *33*, 428–432.
(22) Keller, T.; Krist, T.; Danzig, A.; Keiderling, U.; Mezei, F.; Wiedenmann, A. *Nucl. Instrum. Methods Phys. Res., Sect. A* **2000**, *451*, 474–479.
(23) Wiedenmann, A. *Physica B* **2001**, *297*, 226–233.
(24) Wiedenmann, A. In *Lecture Notes in Physics*; Odenbach, S., Ed.; Springer: Berlin, 2002, pp 33−61.
(25) Pezron, I.; Djabourov, M.; Leblond, J. *Polymer* **1991**, *32*, 3201–3210.
(26) Debye, P.; Bueche, A. M. *J. Chem. Phys.* **1948**, *16*, 573.
(27) Benguigui, L.; Boue, F. *Eur. Phys. J. B* **1999**, *11*, 439–444.
(28) Vesperinas, A.; Eastoe, J.; Wyatt, P.; Grillo, I.; Heenan, R. K. *Chem. Commun.* **2006**, *4407*, 4409.
(29) Bartlett, P.; Ottewill, R. H. *J. Chem. Phys.* **1992**, *96*, 3306–3318.
(30) Hayter, J. In *Physics of Amphiphiles: Micelles, Vesicles and Microemulsions*; DeGiorgio, V., Corti, M., Eds.; North Holland: Amsterdam, 1983, pp 59−93.
(31) Hayter, J. B.; Penfold, J. *Mol. Phys.* **1981**, *42*, 109–118.

Table 2. Parameters Resulting from the Simultaneous Fit of SANSPOL and SAXS Intensities

structure	parameter	SANSPOL results	SAXS results
MagNP	volume fraction	$0.00227 \pm 9.9 \times 10^{-5}$	
	average radius	38.6 ± 1.4 Å	36.7 ± 0.3 Å
	polydispersity	0.419 ± 0.004	0.498 ± 0.042
	nuclear/atomic SLD	$5.77 \times 10^{-6} \pm 0.3 \times 10^{-8}$ Å^{-2}	3.98×10^{-5} Å^{-2}
	magnetic SLD	$6.8 \times 10^{-7} \pm 2 \times 10^{-8}$ Å^{-2}	
gel	I_0 Lorentz	1.21 ± 0.05 cm^{-1}	
	ξ	42.8 ± 9.8 Å	42.8 ± 17.7 Å
	I_0 excess	63.1 ± 7.4 cm^{-1}	
	a	158.4 ± 9.0 Å	149.0 ± 22.3 Å
	solvent SLD	$6.36 \times 10^{-6} \pm 9 \times 10^{-8}$ Å^{-2}	9.33×10^{-6} Å^{-2}
	incoherent bkg	0.1009 ± 0.0006 cm^{-1}	

The fitting results reported in Table 2 show that the size distribution of the MagNPs, as well as both the magnetic and the nuclear SLDs, are in very good agreement with previously published results.[14] Furthermore, the MagNPs′ volume fraction is consistent with the concentration of nanoparticles as obtained by thermogravimetric analysis (TGA; see Supporting Information), indicating that the nanoparticles are homogeneously distributed into the gel matrix.

The mesh and inhomogeneity domain size of the gel structure are about 4 and 16 nm, respectively. These values show a very good agreement with previously reported results for similar kind of gelatin structures,[27,28] confirming that the investigated samples consist of a gel matrix where the MagNPs are embedded and distributed thoroughly the gel matrix.

SAXS. The nanocomposite structure of the nanomagnetic gel was also investigated by means of SAXS. The sample was the same one used for SANSPOL analysis, but H_2O was used instead of D_2O. In the SAXS experiment, the electronic density of the nanoparticles is so high (with respect to both water and the gel structure) that the scattering arising from them nearly overrules all the other contributions, that is, only the nanoparticles can be seen. SAXS intensity distribution is shown in Figure 4, together with the curve obtained by fitting experimental results according to the same model used for the SANSPOL data. Furthermore, SANSPOL results were used as starting values in the SAXS fitting procedure. The parameter values resulting from the fit are reported in Table 2, showing a very good agreement with results

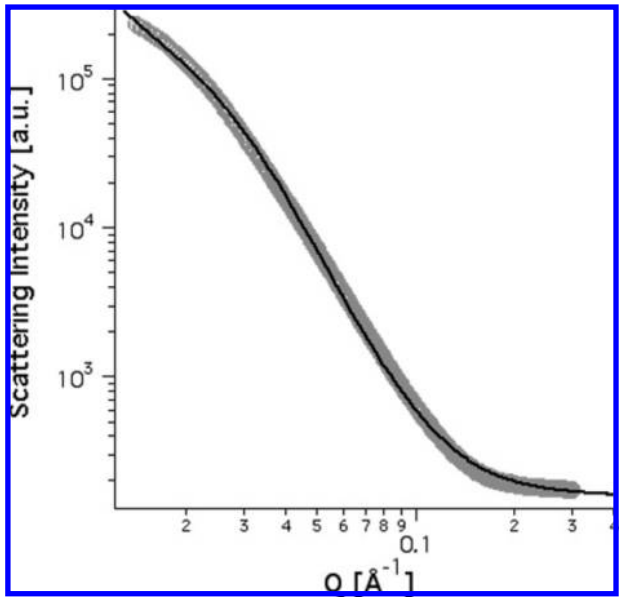

Figure 4. SAXS curve (gray circles) of the MagGel sample together with the fit result (black solid line).

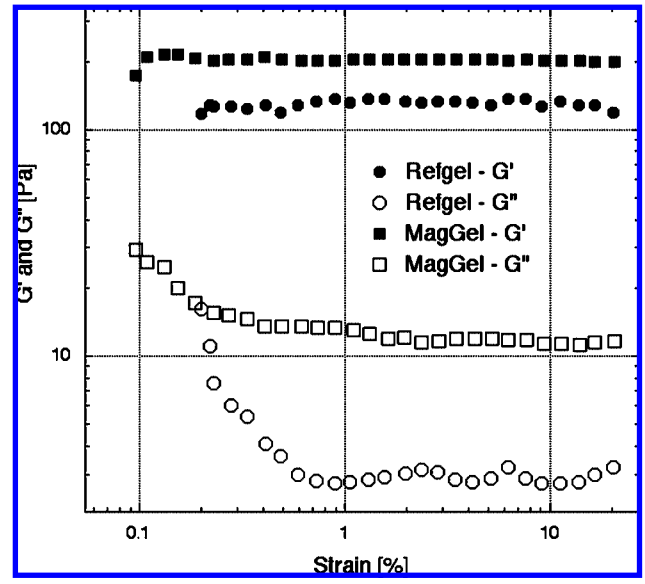

Figure 5. Amplitude sweep results for samples RefGel and MagGel at an angular frequency of 1 s^{-1}.

obtained by SANSPOL. Since SAXS results are in arbitrary units, the values of MagNP volume fraction, *I_0-Lorentz*, *I_0-excess*, and incoherent background, are meaningless parameters, while the SLD values were fixed according to their theoretical values for X-rays. The results obtained by SAXS, reported in Table 2, are in excellent agreement with those obtained from SANSPOL and confirm both the geometrical features of the nanoparticle and their distribution into the gel.

Rheology. The rheological properties of samples RefGel and MagGel were investigated. In order to ensure that all measurements were performed within the linear viscoelastic region, the values of the stress amplitude were checked by means of an amplitude sweep test. Figure 5 shows amplitude sweep results for samples RefGel and MagGel at an angular frequency of 1 s^{-1}.

Considering that the storage modulus G' and the loss modulus G'' are independent from the applied strain above a critical value of almost 1%, it is possible to apply the linear viscoelasticity theory to analyze the results.

Dynamic mechanical properties of samples RefGel and MagGel were investigated by frequency sweep oscillation tests. Figure 6 shows the storage modulus G', the loss modulus G'', and the complex viscosity η^* dependency on the frequency at a constant strain of 5%. The storage modulus of the RefGel sample is always larger than the loss modulus, and no crossover between the G' and G'' curves is observed within the range of the accessible frequencies; this behavior is typical of solid-like materials with infinite relaxation time. Furthermore, Figure 6 indicates that, while G' is almost constant, G'' shows a minimum at intermediate frequencies. Upon the addition of the MagNPs, the relative trend of the shear moduli remains almost the same, but their values increase. In particular, a more elastic response is observed: the G' average value passes from almost 80 Pa for the reference sample to almost 200 Pa for the MagGel sample. This trend is the same observed in the amplitude sweep measurements. More than discussing the absolute values, it is important to stress that the reference and nanocomposite gels show very similar viscoelastic behavior, indicating that the rheological properties are very similar. Furthermore, being for both the investigated samples the G' values almost independent from the frequency of the applied stress, the average values of G' can be considered

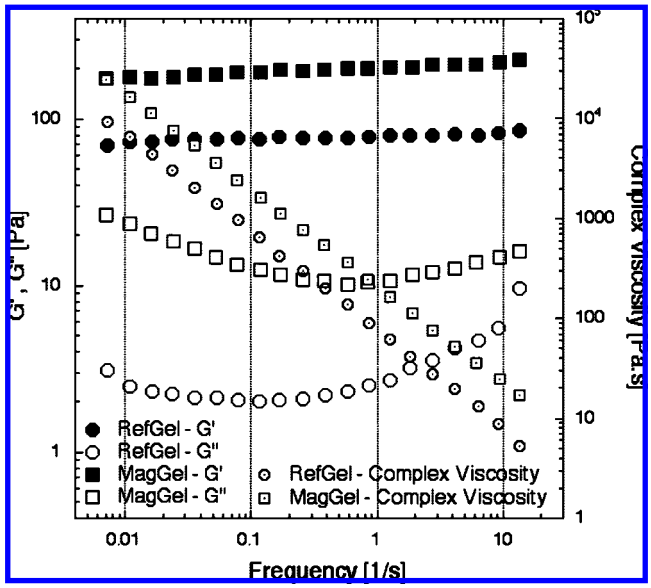

Figure 6. Storage moduli G', the loss moduli G'', and the complex viscosities η^* dependency on the frequency at a constant strain of 5% for samples RefGel and MagGel.

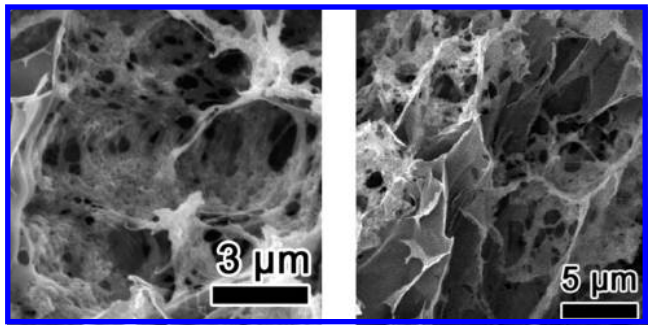

Figure 7. SEM micrographs of the MagGel sample at two different magnifications.

equal to the intrinsic elastic shear modulus of the gel G[32] and we can correlate G to the entanglement density ρ_e as follows: $G = \rho_e k_B T$. An increase in the elastic modulus G' values indicates an increase in the entanglement density induced by the nanoparticles, even if the rheological behavior remains very similar.[33] This effect can be attributed to the anchoring of the PAAm/PEO chains to the MagNP's surface, which plays the role of "entanglement sites" and increases the structure of the gel.

As introduced in the Experimental Section, even if the rheology results cannot be quantitatively discussed because of the sample preparation procedure, it is possible to conclude that the viscoelastic properties of the reference gel are qualitatively retained in the nanocomposite gel where the nanoparticles loading induces an increase of the strength of the 3D network, further confirmed by the increase of the complex viscosity η^* (for the MagGel is almost double the RefGel).

SEM. Two representative SEM pictures are shown in Figure 7. The presence of the MagNPs (very electron-rich) is responsible for the brightest parts of the images. These nanoparticle aggregates are also identifiable by the irregular shape, while the pure gel appears as darker gray areas (less electron-rich) with a smooth surface. The structure is very porous, with pores having diameter

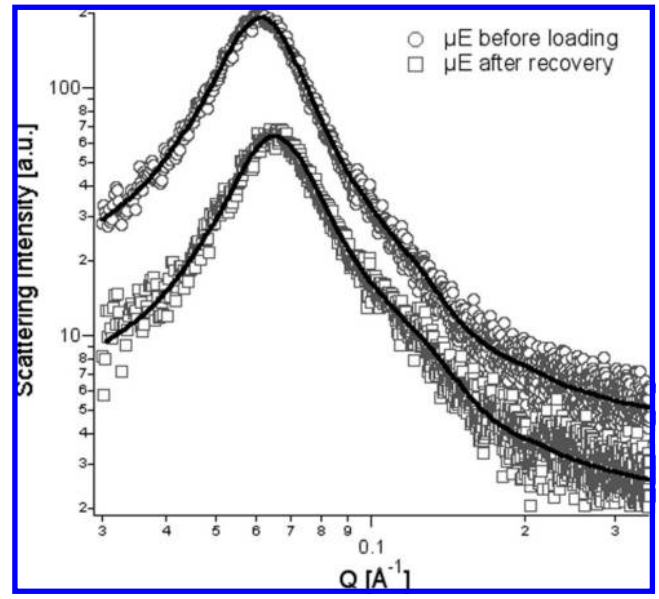

Figure 8. SAXS curves of the μE before uploading it on MagGel and after its recovery. Curves resulting from the fitting routine are shown as solid lines. For the sake of clarity, both experimental data and fitting results are offset (+50 au).

Table 3. Parameters Resulting from the Fit of SAXS Intensities on μEs

coefficient	before loading	after recovery
r_c, core radius	28.8 ± 1.4 Å	25.3 ± 2.4 Å
core polydispersity	0.28 ± 0.01	0.29 ± 0.03
t, shell thickness	5.3 ± 0.5 Å	5.7 ± 0.9 Å
Z, micellar charge	28.1 ± 1.3	27.4 ± 2.7

from hundreds of nanometers to several microns. Note that this porous structure enables this material to work as a "container" for other substances such as, for example, solutions or μEs.[8]

Microemulsions. In order to demonstrate the efficiency of these nanomagnetic sponges to act as containers for water-based formulations, we uploaded a μE widely used in the cleaning of damaged works of art.[34,35] The μE was prepared as previously described[34,35] and it was then uploaded simply by dipping the MagGel xerogel in the μE. The μE was finally recovered from the μE-loaded MagGel by applying an anisotropic magnetic field with the aid of a permanent magnet (maximum field ca. 1.44 T). In the presence of a magnetic field, the MagGel shrinks as a result of its magnetic nature, releasing its liquid content. Both the μEs (before uploading and after recovery) were studied by means of SAXS to verify whether the μE maintains its nanostructure or the preferential adsorption of its constituents to the gel suprastructure destroys it. Figure 8 shows the results, together with the fitting obtained according to a model introduced by Chen and co-workers.[36] Without going into the fitting details (see Supporting Information), the μE is modeled as electrostatically charged polydisperse core−shell spheres (t being the thickness of the shell, r_c being the average radius of the core, and Z being the effective charge number per micelle). According to the values of the coefficients resulting from the fit (see Table 3), the two μEs (before the uploading and after the recovery) are almost identical. The only difference is the slight decrease in the size of the core radius after recovery. This is probably due

(32) Raghavan, S. R.; Kaler, E. W. *Langmuir* **2001**, *17*, 300–306.
(33) Schubert, B. A.; Kaler, E. W.; Wagner, N. J. *Langmuir* **2003**, *19*, 4079–4089.
(34) Carretti, E.; Salvadori, B.; Baglioni, P.; Dei, L. *Studies in Conservation* **2005**, *50*, 1–8.
(35) Carretti, E.; Dei, L.; Baglioni, P. *Langmuir* **2003**, *19*, 7867–7872.
(36) Liu, Y. C.; Baglioni, P.; Teixeira, J.; Chen, S.-H. *J. Phys. Chem.* **1994**, *98*, 10208–10215.

to the weak interaction between the organic part of the μE (i.e., the solvents constituting the droplets) and the hydrophobic regions of the gel. This corresponds to a decrease in the hydrophobic content of the μE, which is expected to produce a decrease in the droplets' size.

Conclusions

In this paper we report the formulation and the characterization of a nanomagnetic sponge where the mechanical and hydrophilic properties of acrylamide gels are combined with the magneto-responsive properties of MagNPs. A linear linker consisting of an ethylene glycol core, a carboxylic group at each extremity of the linker, and two polymerizable anchor points was synthesized by coupling PEG and MA. Such a linear linker was used to embed the MagNPs into the acrylamide-based gel network.

The nanocomposite sponge was studied by means of SAXS and SANSPOL. In particular, this last technique is extremely well-suited in the characterization of nanoscaled magnetic objects and allowed us to reveal both the gel structure and the nanoparticle arrangement within.

The mechanical properties of this novel nanocomposite material were investigated by means of rheological measurements, showing that the viscoelastic properties of acrylamide gels are qualitatively retained in the nanomagnetic gel, where the presence of nanoparticles only induces an increase in the mechanical strength of the 3D network. Hydrophilic properties were also studied, demonstrating that the magnetic nanosponge can be efficiently used to load a large amount of water: in fact, the nanocomposite gel can be used to load water-based formulations up to about 9 times its dry weight. This is made possible thanks to its highly porous structure, as shown by the SEM results. Moreover, the magnetic sponge can be magnetically squeezed, dried, and swollen again.

Finally, it is important to emphasize that such nanomagnetic gel structure opens up new perspectives in the use of smart materials in applications where water-based formulations must be locally and selectively applied and cleanly removed. Here, the uploading and recovery of an oil-in-water μE was studied, showing the effectiveness of such a nanomagnetic sponge as an active container. In particular, we have already shown how this approach can be successfully applied in the cleaning of works of art.[8]

This new nanomagnetic gel is a clear example of how the bottom-up approach represents a powerful tool in the design of materials with enhanced functionalities.

Acknowledgment. Financial support from Ministero dell'Istruzione, Università e della Ricerca Scientifica (MiUR, Grant PRIN-2007) and Consorzio Interuniversitario per lo Sviluppo dei Sistemi a Grande Interfase, CSGI, is gratefully acknowledged.

Supporting Information Available: Details about the small-angle scattering fitting procedure (SANSPOL and SAXS) and the TGA of the sample analyzed by SANSPOL are available as Supporting Information. This material is available free of charge via the Internet at http://pubs.acs.org.

LA802425K